Dynamic Lorentz microscopy of micromagnetic structure in magnetic tunnel junctions

Justin M. Shaw,[a] Roy Geiss, and Stephen Russek
National Institute of Standards and Technology, Boulder, Colorado 80305

(Received 26 June 2006; accepted 22 September 2006; published online 20 November 2006)

Lorentz microscopy was used to study the micromagnetic structure and magnetization reversal in magnetic tunnel junctions (MTJs) fabricated with different processing conditions including a preoxidation process. The authors find that the free layer in a MTJ has considerably more disorder than that seen in an isolated magnetic layer. The disorder changes with anneals that set the exchange bias, suggesting that the disorder arises from the antiferromagnetic layer and is transferred to the free layer by magnetostatic Néel coupling. The disorder and time-dependent fluctuations in the magnetic structure provide a foundation for understanding several sources of $1/f$ noise in MTJs. © *2006 American Institute of Physics*. [DOI: 10.1063/1.2385207]

Magnetic tunnel junction (MTJ) based devices have many applications in existing and developing technologies such as disk drive read heads, low-field magnetic sensors, and magnetic random access memory (MRAM). Understanding and controlling the micromagnetic structure of MTJs and their time-dependent fluctuations are critical to advancing these technologies. In low-field sensor technologies, extremely soft free layers without the presence of any magnetic fluctuations are needed because these fluctuations introduce $1/f$ noise and degrade device performance.[1] In addition to fluctuations, magnetic homogeneity across a production wafer's surface is important for MTJ device applications to minimize performance variations from device to device.[2] Micromagnetic structure may be particularly important in determining switching distributions in MRAM. Parasitic magnetic coupling—such as Néel or "orange-peel" coupling—is also undesirable due to the introduction of an offset field in the reversal of the free magnetic layer.

Using dynamic Lorentz microscopy techniques we studied MTJ structures designed for low-field sensor technology where $\mathrm{pT}/\sqrt{\mathrm{Hz}}$ sensitivity is desired. We investigated several process variations, including a preoxidation process.[3,4] We use a 22 nm free layer which is required in our patterned sensors to provide a nonhysteretic response along the hard axis. This free layer thickness is larger than those used for other applications such as read heads and MRAM. Free layers as thick as 13 nm show an undesirable hysteretic response along the hard axis unsuitable for such low-field sensors.[5,6] We directly observe and compare processing effects on the micromagnetic structure, magnetization reversal, and time-dependent magnetic fluctuations in these MTJs. The direct observation of micromagnetic structure and time-dependent magnetic fluctuations for different processing conditions provides a foundation for understanding $1/f$ noise and device-to-device variations.

Our MTJ structures were deposited on 40 nm Si_3N_4 membrane windows that had dimensions of $100\times100\ \mu m^2$. The MTJ thin-film stacks were held in a 15 mT magnetic field during deposition in a dc magnetron sputtering system. The MTJ structure is as follows: 5 nm Ta/5 nm Cu/10 nm $Ir_{20}Mn_{80}$/3 nm $Co_{90}Fe_{10}$/1.8 nm Al_2O_3/2 nm $Co_{90}Fe_{10}$/20 nm $Ni_{80}Fe_{20}$/5 nm Ta. The $Ir_{20}Mn_{80}$ layer is an antiferromagnet that exchange couples to the $Co_{90}Fe_{10}$ layer to pin its magnetization along a specific direction. The $Co_{90}Fe_{10}/Ni_{80}Fe_{20}$ forms the magnetically soft free layer. The Al_2O_3 layer was made by depositing 1.2 nm Al and exposing this layer to an O_2 plasma for 100 s at 0.4 Pa (3 mTorr), which results in a 1.8 nm Al_2O_3 tunnel barrier. For the preoxidized sample, we exposed the bottom (pinned) $Co_{90}Fe_{10}$ layer to 0.4 Pa O_2 for 30 s prior to depositing the Al_2O_3. It was found by Egelhoff, Jr. *et al.*[3] that the properties of the preoxidized MTJs do not vary significantly with O_2 exposure time due to a self-passivation/limiting process. *Ex situ* atomic force microscopy measurements of the entire MTJ structure reveal that the root-mean-square surface roughness from the preoxidized $Co_{90}Fe_{10}$ is reduced by 28% relative to the identical MTJ structures without the preoxidized process. This is consistent with x-ray reflectometry measurements performed by Egelhoff, Jr. *et al.*[4] which show a decreased interface roughness with the preoxidation process. Following deposition, we annealed some of our MTJs at 280 °C for 60 min in a 100 mT magnetic field. This annealing process increases the tunneling magnetoresistance (TMR) from ≈15% to ≈45% in these layers and increases the pinning field from ≈350 to ≈700 mT. The annealing process alone does not have a significant effect on the surface roughness.

Lorentz microscopy was performed in a 200 kV transmission electron microscope operated with the objective lens turned off. Image magnification and focus were performed with an objective minilens. Magnetic contrast was achieved by use of the Fresnel method whereby the image was slightly overfocused or underfocused. For all data reported here, dynamic imaging was performed with an image capture rate of 2 Hz, although we have demonstrated imaging up to 30 Hz.

To rule out any stress induced effects on the magnetic properties caused by growth on the thin Si_3N_4 membranes, we used a longitudinal magneto-optic Kerr effect system with a 50 μm focused beam to compare the magnetic properties on the membrane and on the rigid substrate surrounding the membrane. The magnetic properties were identical at all locations.

Alternating gradient magnetometry (AGM) measurements taken along the easy axis of the unannealed, annealed,

[a]Electronic mail: justin.shaw@nist.gov

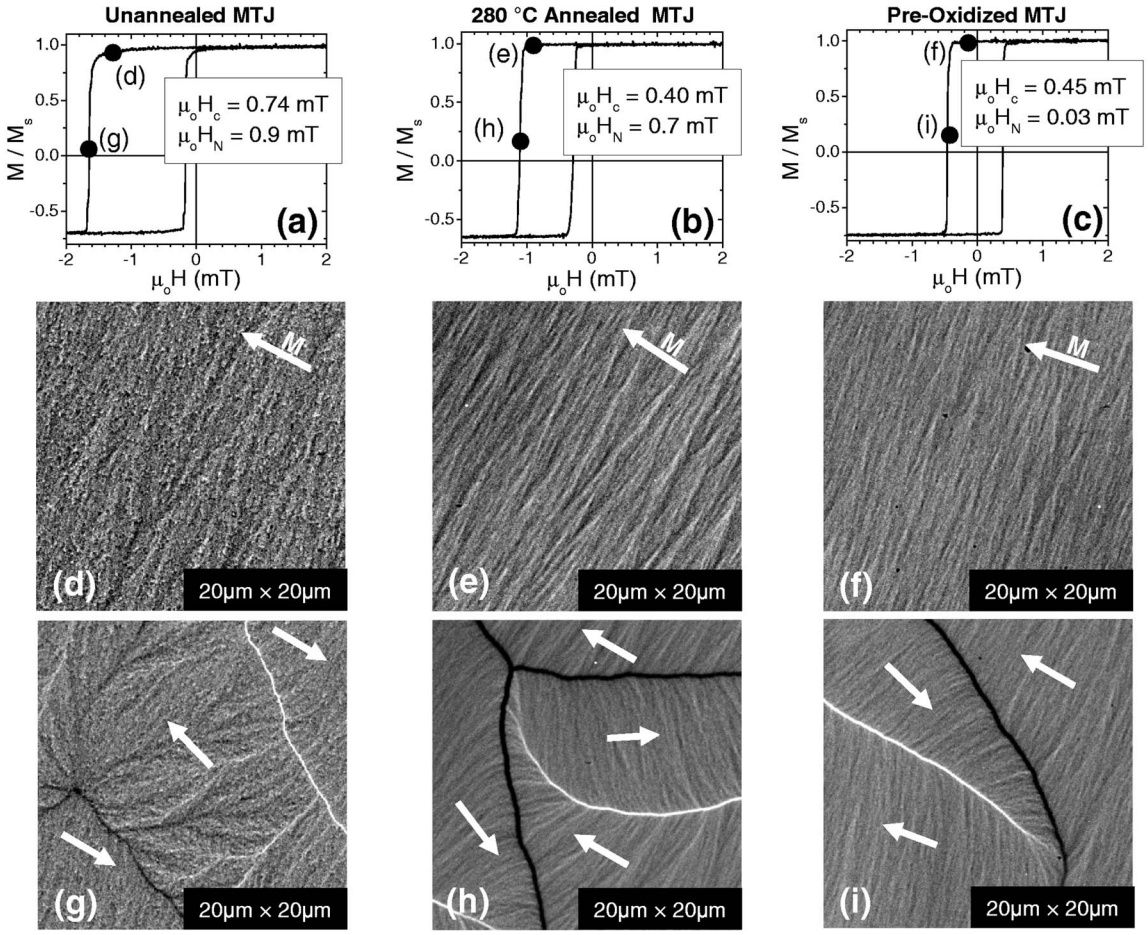

FIG. 1. AGM hysteresis loops along the easy axis of the free layer for the (a) unannealed, (b) annealed, and (c) preoxidized MTJs. Lorentz microscopy images taken prior to magnetization reversal for the (d) unannealed, (e) annealed, and (f) preoxidized MTJs, and images taken during magnetization reversal for the (g) unannealed, (h) annealed, and (i) preoxidized MTJs. For simplicity, the arrows indicate the direction of the idealized magnetization to show the reversal state. The actual direction of the magnetization is significantly more complex and nonuniform.

and preoxidized (also annealed) samples are shown in Figs. 1(a)–1(c), respectively. The coercive field (H_c) and the Néel coupling field (H_N) calculated from these loops are included in the figures. The most striking result is the reduction of the Néel coupling field to 0.03 mT due to the preoxidation process.

Lorentz images taken just prior to magnetization reversal are shown in Figs. 1(d)–1(f) and those taken during magnetization reversal are shown in Figs. 1(g)–1(i) for the unannealed, annealed, and preoxidized MTJs, respectively. The point during the reversal process at which each image was captured is indicated in the AGM loops. The unannealed MTJ overall displays a highly nonoriented rippled magnetic structure prior to reversal and undergoes a significantly more chaotic reversal process. Magnetic ripple refers to small local variations of the magnetization within the layer and can be a source of Barkhausen jumps, which cause low-frequency noise in devices. In fact, many magnetic fluctuations and Barkhausen jumps occurred in static fields. Figure 2(a) shows a small 0.2 μm structure that jumps back and forth between two positions while being held in a static magnetic field. A single Barkhausen jump is also shown in Fig. 2(b). These are excellent examples of how Lorentz microscopy can be used to directly observe sources of noise in device structures.

During reversal on the unannealed MTJ in Fig. 1(g), the domain wall boundary is jagged, with an intense ripple structure surrounding it. This reversal behavior is undesirable because it can lead to variation in switching behavior from

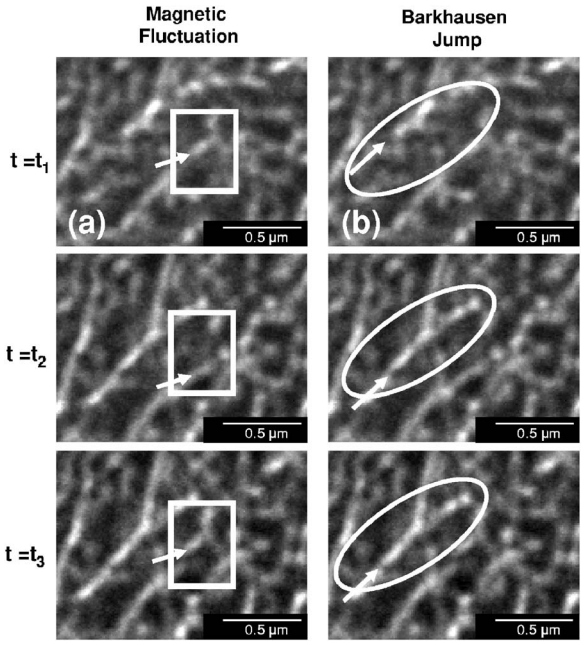

FIG. 2. Series of Lorentz images showing (a) a 0.2 μm magnetic fluctuation and (b) a single 1 μm Barkhausen jump occurring between t_1 and t_2. The total time interval from t_1 to t_3 is approximately 10 min.

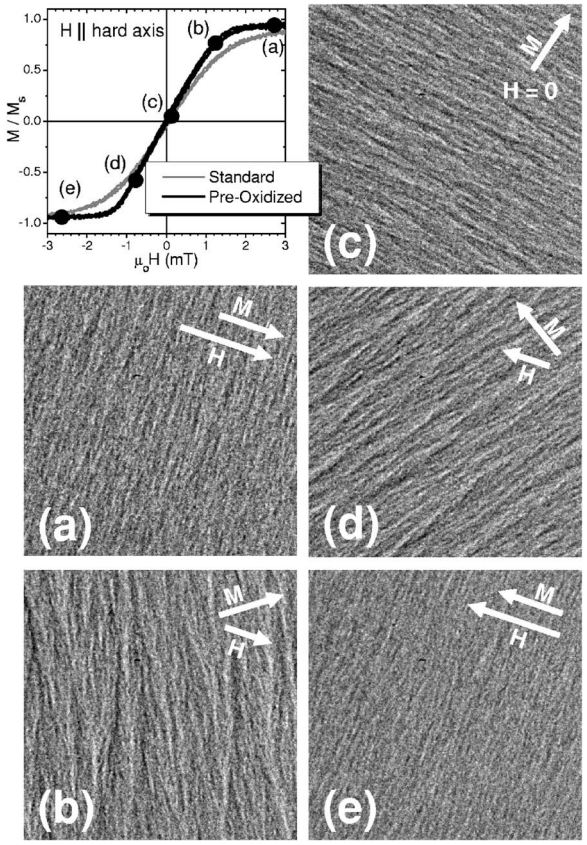

FIG. 3. AGM data taken along the hard axes for the standard annealed (gray) and preoxidized (black) MTJs. Several Lorentz images are given [(a)–(e)] at various points along the preoxidized curve as indicated in the plot. All Lorentz images are 20×20 μm^2.

device to device. The AGM loop for this sample also indicates a larger value for the coercive field and a more gradual reversal, consistent with a higher concentration of magnetic defects and magnetic inhomogeneity.

The micromagnetic structure is greatly improved when the MTJ is annealed. This result is consistent with the 300% increase in TMR and the 200% increase in the pinning field measured in our devices after undergoing the annealing process. Figures 1(e) and 1(h) show smoother domain boundaries with a reduced intensity of magnetic ripple. In addition, the ripple structure becomes more longitudinal in orientation where the ripple is perpendicular to the average magnetization. This longitudinal quality was previously observed in stand-alone Permalloy thin films and in spin-valve structures.[7–11] The magnetic ripple is further reduced for the preoxidized MTJ, consistent with the measured reduction in the Néel coupling, and further increased TMR.[3] Fourier transform analysis of the ripple structure for the MTJ with and without the preoxidation process shows that the preoxidized MTJ has both a smaller average wavelength and a lower intensity. Finer wavelength is desirable because the Barkhausen jumps in these structures are on the order of the average ripple wavelength.

The preoxidation process also has a profound effect on the hard axis response, as shown in Fig. 3. The preoxidized MTJ is significantly more linear up to saturation. This linear response, with no coercive field, is extremely desirable in low-field magnetic sensor technology. Lorentz images taken with the magnetic field directed along the hard axis shows a full 180° rotation of the magnetic ripple. A series of images taken during this magnetization rotation from positive saturation to negative saturation is shown in Fig. 3 for the preoxidized MTJ. The magnetic ripple is most intense when the magnetization is oriented at a large angle relative to the applied field. In the full 2 Hz dynamic image sequence, a large amount of discrete jumps in the micromagnetic structure occurred throughout the entire 180° rotation. In a device, these discrete jumps would result in signal noise. Thus, minimization of this phenomenon and achieving a finer micromagnetic structure are critical, especially in low-field sensors.

It is important to note that even in the MTJs with preoxidation, the disorder and ripple are considerably larger than those for a sample with only the free layer present. The micromagnetic structure must be in the free layer, since the AGM loops clearly indicate that the pinned layer does not change over the fields used in the Lorentz studies. This study suggests that the disorder originates in the exchange bias layer and is transferred to the free layer by local magnetostatic coupling. The annealing procedure changes the interfacial properties near the tunnel junction (as indicated by the change in TMR) and the exchange coupling (as indicated by the increase in exchange bias field) but does not significantly affect the magnetic properties of the free layer. Although the MTJs studied in this work are designed for low-field sensor technology, these fundamental effects would also be present in MTJ structures being developed for other technologies where thinner free layers are implemented since they originate in the pinned layer.

In summary, we have used Lorentz microscopy to study the real-time micromagnetic behavior of several MTJ thin-film multilayers. The quality of the micromagnetic structure and magnetization reversal process was found to be highly dependent on processing conditions. MTJ structures undergoing a preoxidation step show a dramatic decrease in the magnetic ripple, a smoother magnetic reversal, and a decreased Néel coupling field. Finally, dynamic imaging revealed the presence of small discrete jumps and fluctuations in the micromagnetic structure. This study indicates that the multilayer MTJ structure can introduce considerable disorder in the magnetic layers which can in turn lead to noise in devices.

The authors are grateful to Bill Rippard, Dave Pappas, and Bill Egelhoff for their support and fruitful discussions.

[1] L. Jiang, E. R. Nowak, P. E. Scott, J. Johnsom, J. M. Slaughter, J. J. Sun, and R. W. Dave, Phys. Rev. B **69**, 054407 (2004).
[2] E. Y. Chen, R. Whig, J. M. Slaughter, D. Cronk, J. Goggin, G. Steiner, and S. Tehrani, J. Appl. Phys. **87**, 6061 (2000).
[3] W. F. Egelhoff, Jr., R. D. McMichael, C. L. Dennis, M. D. Stiles, A. J. Shapiro, B. B. Maranville, and C. J. Powell, Appl. Phys. Lett. **88**, 162508 (2006).
[4] W. F. Egelhoff, Jr., P. J. Chen, R. D. McMichael, C. J. Powell, R. D. Deslattes, F. G. Serpa, and R. D. Gomez, J. Appl. Phys. **89**, 5209 (2001).
[5] M. Tondra, J. M. Daughton, C. Nordman, D. Wang, and J. Taylor, J. Appl. Phys. **87**, 4679 (2000).
[6] D. Wang, J. M. Daughton, Z. Qian, C. Nordman, M. Tondra, and A. Pohm, J. Appl. Phys. **93**, 8558 (2003).
[7] Harrison W. Fuller and Murray E. Hale, J. Appl. Phys. **31**, 238 (1960).
[8] Horst Hoffmann, J. Appl. Phys. **35**, 1790 (1964).
[9] J. N. Chapman and M. R. Scheinfein, J. Magn. Magn. Mater. **200**, 729 (1999).
[10] C. K. Lim, J. N. Chapman, M. Rahman, A. B. Johnston, and D. O. O'Donnell, J. Appl. Phys. **95**, 1510 (2004).
[11] A. Gentils, J. N. Chapman, G. Xiong, and R. P. Cowburn, J. Appl. Phys. **98**, 053905 (2005).